Characterization of two genetic variants of $Na_v1.5$-Arginine 689 found in patients with cardiac arrhythmias

Valentin Sottas[1], Jean-Sébastien Rougier[1], Florian Jousset[2], Jan P. Kucera[2], Anna Shestak[3], Leonid M. Makarov[4], Elena V. Zaklyazminskaya[3]*, Hugues Abriel[1]*

[1]Department of Clinical Research, University of Bern, Switzerland
[2]Department of Physiology, University of Bern, Switzerland
[3]Russian Research Centre of Surgery RAMS, Laboratory of Medical Genetics, Moscow, Russia
[4]Center for Syncope and Arrhythmias in Children and Adolescents FMBA, Moscow, Russia

Short title: $Na_v1.5$-Arg689 in arrhythmias

Funding: The groups of EVZ and HA are supported by a grant for scientific co-operation between Eastern Europe and Switzerland by the Swiss National Science Foundation (SCOPES #IZ73Z0_128016). This work was also supported by a grant from the Swiss National Science Foundation to HA (310030B_135693). FJ is supported by the European Union (European Network for Translational Research in Atrial Fibrillation (EUTRAF) FP7 grant).

*Correspondence to:

Dr. Hugues Abriel, MD PhD
University of Bern,
Department of Clinical Research
Murtenstrasse 35, 3010 Bern, Switzerland
Phone: 41-31-6320928
Fax: 41-31-6320946
Email: Hugues.Abriel@dkf.unibe.ch

Dr. Elena V. Zaklyazminskaya, MD PhD
Russian Research Centre of Surgery
RAMS, Laboratory of Medical Genetics,
Moscow, Russia
Phone: 7-499-2485495
Fax: 7-499-2485495
Email: zhelene@mail.ru

Abstract

Hundreds of genetic variants in *SCN5A*, the gene coding for the pore-forming subunit of the cardiac sodium channel, $Na_v1.5$, have been described in patients with cardiac channelopathies as well as in individuals from control cohorts. The aim of this study was to characterize the biophysical properties of two naturally-occurring $Na_v1.5$ variants, p.R689H and p.R689C, found in patients with cardiac arrhythmias and in control individuals. In addition, this study was motivated by the finding of the variant p.R689H in a family with sudden cardiac death (SCD) in children.

When expressed in HEK293 cells, most of the sodium current (I_{Na}) biophysical properties of both variants were indistinguishable from the wild-type (WT) channels. In both cases, however, a ~2-fold increase of the tetrodotoxin-sensitive late I_{Na} was observed. Action potential simulations and reconstruction of pseudo-ECGs demonstrated that such a subtle increase in the late I_{Na} may prolong the QT interval in a non-linear fashion. In conclusion, despite the fact that the causality link between p.R689H and the phenotype of the studied family cannot be demonstrated, this study supports the notion that subtle alterations of $Na_v1.5$ variants may increase the risk for cardiac arrhythmias.

Key words: Cardiac sodium channel, $Na_v1.5$, long QT syndrome, Brugada Syndrome, Sudden Cardiac Death

Introduction

Since 1995, hundreds of genetic variants in *SCN5A*, the gene coding for the pore-forming subunit of the cardiac sodium channel, $Na_v1.5$, have been reported (1). The vast majority of these variants are single nucleotide polymorphisms (SNPs). In most cases, these variants were found in patients and families with distinct, inherited forms of cardiac arrhythmias, in particular the congenital long QT syndrome (LQTS) type 3 and Brugada syndrome (BrS) (2). In some cases, however, patients and families may display more than one phenotype which has led to the concept of an "*SCN5A*-overlap syndrome" (3). Only a small fraction of these $Na_v1.5$ variants has been functionally characterized by expressing them in cellular expression systems (4) or by generating genetically-modified mouse models (5, 6). More recently, induced pluripotent stem cell-derived cardiomyocytes from patients with mutated *SCN5A* alleles were also used to investigate their pathogenicity (7). Other recent studies (8, 9) have demonstrated that *SCN5A* is a polymorphic gene, and as a consequence, one of the main challenges for this field is to distinguish between rare but benign (silent SNPs) and pathogenic ones. There exists different approaches to address this clinically-relevant question (10). However, molecular and biophysical characterization of $Na_v1.5$ channels that are heterologously expressed in mammalian cells, remains one of the most informative methods to investigate the pathogenicity of naturally-occurring variants.

In the present study, we characterized two naturally-occurring *SCN5A* variants of the same locus, p.R689H (c.2066G>A) and p.R689C (c.2065C>T). When analyzed with the "Sorting Tolerant From Intolerant" (SIFT) algorithm (11), p.R689H was classified as "damaging", while the Polyphen software (12) classified it as "benign"; p.R689C was classified as "damaging" by SFIT and "possibly damaging" using Polyphen (12). These

two variants were already reported several times in the literature (8, 13-17) (summarized in Table 1), either in patients with LQTS or BrS, or in individuals from control cohorts. In this study, the p.R689H variant was found in five females from a single Russian family with a history of sudden cardiac death (SCD) and cardiac conduction defect (published in Russian language (18)). Notably, this p.R689H variant has been recently studied, since it was found in one asymptomatic Chinese patient with both short QT interval and an ECG with a BrS pattern (13). When transfected in HEK293 cells, the p.R689H *SCN5A* variant did not generate any measurable current (13). The variant p.R689C was previously reported in one patient with LQTS (8), but thus far, no functional analyses have been performed. The variant p.R689H was reported with a very low allelic frequency of 1/12747 in the exome variant server database (19); while the variant p.R689C was absent.

The main objectives of the present study were to investigate the biophysical properties of these two *SCN5A* variants, p.R689C and p.R689H, expressed in HEK293 cells, and to perform simulations of cardiac action potential (AP) and reconstructions of pseudo-ECGs incorporating the observed alterations.

Material and methods

Genetic analyses

DNA samples were extracted from venous blood samples or from paraffin-embedded blocks. Genetic studies were performed according to the declaration of Helsinki. All family members signed an informed consent form. For minors, this was done by their legal representatives. A few family members refused genetic counseling and genetic analyses (individuals II.3 and III.4, Fig.1A). They were informed that this negative decision would not change their medical work-up, and that they could change their opinion at any time. Genetic screening was performed by PCR-based Sanger sequencing of full coding sequences and adjacent intronic areas of the following genes: *SCN5A, TRPM4, HCN2, GJC1, CASQ2, SNTG2, and LMNA*. The sequence of the primers used can be provided upon request. The prevalence of the rare variants was tested in a control group of 115 healthy volunteers (230 chromosomes)..

Transfection and DNA constructs

For electrophysiological studies, HEK293 cells were transiently transfected in T25 flasks with WT, p.R689H, or p.R689C constructs. All transfections included 2.0 µg pIRES-hβ1-CD8 cDNA, encoding the hβ1 subunit and CD8 antigen as a reporter gene. All transfections were performed with a Lipofectamine transfection mix (Sigma) for 18 hours following the manufacturer's instructions. Anti-CD8 beads (Dynal) were used to identify transfected cells, and only decorated cells were analyzed. Mutant constructs were generated using the QuickChange Mutagenesis Kit (Stratagene) and verified by sequencing.

Electrophysiology

Whole-cell currents were measured at room temperature (20-22 °C), using either a VE-2 amplifier (Alembic instruments) or an Axopatch 200B amplifier (Axon CNS) for I_{Na} late current recordings (seal R >5 GΩ). Thirty µM tetrodotoxin (TTX) or extracellular solution perfusion was performed for I_{Na} late current recordings, using a constant flow on the cell. TTX-sensitive traces were obtained by subtracting the trace obtained with a TTX-perfused cell to the trace obtained with the extracellular solution-perfused cell. Each trace is an average of 10 different sweeps. Holding potentials were −100 mV and no leak subtraction was performed. I_{Na} density (pA/pF) was obtained by dividing the peak current by the cell capacitance obtained from the pClamp function. The resistance of pipettes was in the range of 1.3-2.7 MΩ.

Solutions and chemicals

The internal pipette solution was composed of (mM): CsCl 60, aspartic acid 50, $CaCl_2$ 1, $MgCl_2$ 1, HEPES 10, EGTA 11, Na_2ATP 5, pH 7.2 with CsOH; the external solution was composed of (mM): NaCl 50, NMDG-Cl 80, CsCl 5, $CaCl_2$ 2, $MgCl_2$ 1.2, HEPES 10, glucose 5, pH 7.4 with CsOH. The following bath solution (mM): NaCl 130, CaCl2 2, MgCl2 1.2, CsCl 5, HEPES 10, Glucose 5, pH 7.4 with CsOH, was used for late current experiments. Pipettes were filled with the same intracellular solution. Using these solutions, 5 min after rupturing the membrane, we observed no significant alteration of the availability curve and the peak current.

Data analysis

Currents were analyzed with Clampfit software (Axon Instruments, Inc). Data were analyzed using a combination of pClamp 8, Excel (Microsoft), and Prism (GraphPad). To quantify the voltage-dependence of activation and steady-state inactivation, data from

individual cells were fitted with Boltzmann relationship, $y(V_m) = 1/(1+\exp((V_m-V_{1/2})/K))$, where y is the normalized current or conductance, V_m is the membrane potential, $V_{1/2}$ is the voltage at which half of the available channels are inactivated, and K is the slope factor. The voltage values were not corrected for the junction potential offset of ~16-17 mV. Data are represented as mean values ± SEM. Two-tailed Student t-test was used to compare means.

Computer simulations of the I_{Na}, the action potential, transmural conduction, and pseudo-ECGs

The I_{Na} and APs were simulated using the ten Tusscher-Noble-Noble-Panfilov (TNNP) human ventricular cell model (20). In this model, I_{Na} is represented according to a Hodgkin-Huxley formalism,

$I_{Na} = gNa_{max}\, m^3hj\, (V_m–E_{Na})$,

where gNa_{max} is the maximal conductance of I_{Na}, m^3 represents three activation gates, h and j are inactivation gates, V_m is the membrane potential, and E_{Na} is the Nernst potential of sodium. To simulate a late persistent I_{Na}, we considered that a small fraction ε of I_{Na} activates/deactivates but does not inactivate, and modified the I_{Na} formulation as follows:

$I_{Na} = gNa_{max}\, m^3\, ((1–\varepsilon)hj + \varepsilon)\, (V_m–E_{Na})$.

The parameter ε was adjusted to reproduce the ratio of late I_{Na} to peak I_{Na} that was observed experimentally. Using an approach similar to that of Gima and Rudy (21), a 1.5 cm cable of TNNP model cells was constructed to simulate transmural AP propagation. The first third consisted of endocardial cells, the second third of mid-myocardial cells (M cells), and the last third of epicardial cells. The cable was stimulated on the endocardial side (rate: 1 Hz). Gating variables were integrated using the method

of Rush and Larsen and the other model variables used the forward Euler algorithm, with a constant time step of 0.005 ms. The pseudo-ECG was reconstructed according to Plonsey and Barr (22) by computing the extracellular potential (V_e) at a distance of 2 mm from the epicardial end, along the axis of the cable. The end of the QT interval was defined by the intersection of the steepest tangent to the T wave (having the most negative slope) with the isoelectric line.

Results

Clinical description

The clinical description of the cases of three Russian siblings, suffering from unexplained arrhythmias, was recently published (18). Briefly, genetic counseling and DNA diagnostics were performed for a family (Figure 1A) with incidences of sudden death of twin sisters. The first twin (III.1) died suddenly at the age of 4 years and 6 months, and the second twin (III.2), at the age of 5 years and 5 months. The circumstances of the sudden death were similar: the children were running towards their mother after having spent the day at the kindergarten. Both girls died during their first syncope. Post mortem pathological examinations did not reveal any disease, and the final conclusion was SCD of unknown origin for both twins. The proband of this study, which is the youngest sibling (Figure 1A, III.3), had previous cardiac investigations at the age of 1.5 since she presented with fatigue and dyspnea, hyperhidrosis, and several episodes of syncope. The first syncope was at the age of 5 months. Regular follow-up ECG examinations showed progressive conduction disorder (Figure 1B, Table 2). At the age of 1 year and 6 months, a permanent pacemaker (VVI regime, 70 bpm) was implanted. After the first publication of the case, more family members were examined and genetic investigations were performed for the entire family. The mother (II.2), 32 years old (y.o.), had no cardiac complaints. On her ECG, a prolongation of the QTc up to 485 ms, intermittent negative T-waves in leads V_1-V_2, and slow intra-ventricular conduction were registered (Figure 1C). Her sister (II.3) refused all clinical and genetic investigations for herself and for her 14 y.o. son (III.4). One syncope episode had been observed for this boy. The grandmother (I.2) was asymptomatic but also with borderline QTc prolongation (480 ms). Genetic analyses of 5 candidate genes were performed

(see Material and methods). The variant p.R689H (c.2066G>A) in *SCN5A* was found in the proband, the deceased twins, the mother, and grandmother (Figure 1A) in the heterozygous state. This variant was absent from an ethnically-matched cohort of 115 control individuals.

Biophysical properties of p.R689H and p.R689C

I_{Na} recordings of HEK293 cells, transiently transfected with $Na_v1.5$-WT, $Na_v1.5$-p.R689H, or $Na_v1.5$-p.R689C, using a typical current/voltage protocol in patch-clamp experiments, are presented in Figure 2A. No significant changes were observed in the current densities of p.R689H and p.R689C compared to WT (Figure 2B). The voltage-dependence of activation and steady-state inactivation relationships were not altered (Figure 2C). In addition, as depicted in Figure 2D, no significant difference in fast inactivation could be observed. Recovery from inactivation was also studied, and no significant change was observed between both $Na_v1.5$ variants and WT (Figure 2E). Lastly, the onset of slow inactivation was also analyzed, and no significant change was observed (Figure 2F).

Effect of intracellular pH acidification and high-frequency pacing on p.R689H

When stimulated at -20 mV at high frequencies (2 Hz) using 500 ms pulses to mimic tachycardia, $Na_v1.5$-WT and p.R689H peak currents were decreased to about 50% after 20 stimuli (Figure 3A). Figure 3B and 3C show $Na_v1.5$-WT and p.R689H peak current decreases at different stimuli with intracellular physiological (7.2) and acidotic (6.7) pH, respectively. Decreases of 0.46%±0.05 and 0.47%±0.04 were obtained for $Na_v1.5$-WT and the p.R689H variant, respectively, at physiological pH at the twentieth stimulus. At

acidotic pH, decreases of 0.46%±0.03 and 0.45%±0.03 were obtained at the twentieth stimulus for $Na_v1.5$-WT and the p.R689H variant, respectively.

Variants p.R689H and p.R689C increase the late I_{Na}

The late I_{Na} was analyzed using a depolarization step to -20 mV at a duration of 300 ms (see inset in Figure 4A). Examples of three TTX-sensitive traces for $Na_v1.5$-WT, p.R689H, and p.R689C are depicted in Figure 4A. Both p.R689H and p.R689C variants increased the late I_{Na}, as illustrated in Figure 4B at physiological pH 7.2. The values for the ratio of late I_{Na} / peak current were 0.095% ± 0.01 for WT, 0.19% ± 0.03 for p.R689H, and 0.16% ± 0.02 for p.R689C (Table 3). The differences were significant for both variants ($P<0.05$). The p.Y1795C variant (23) was used as a control to study the late current; previously published results were reconfirmed (0.50% ± 0.04 of the peak current, n=5). No change in the amplitude of the late I_{Na} for p.R689H was observed when using an acidotic intracellular solution (pH 6.7) when compared to pH 7.2 (Figure 4C). p.R689C was not studied with an intracellular acidotic solution, since we did not expect any differences with this amino acid substitution.

Computational study

In the modified I_{Na} formulation of the TNNP model, setting ε (see Material and Methods) to 0.00075 and 0.0015 produced a late I_{Na} with respective amplitudes of 0.1% and 0.2%, relative to peak $I_{Na,}$ which were comparable to the findings of the experiments (Figure 4). These values of ε did not change $V_{½}$ or the slopes of activation and steady-state inactivation curves (see Table 3). To investigate the effects of increasing levels of late I_{Na} on repolarization, simulations of transmural conduction were run and pseudo-ECGs

were reconstructed, using the modified TNNP model with increasing values of ε. As shown in Figure 5A, increasing ε from 0 to 0.00075 (0.1% late I_{Na}) prolonged the reconstructed QT interval. Because the relationship between QT prolongation and late I_{Na} was nonlinear (Figure 5B), a further increase of ε to 1.5 times these values (mimicking a heterozygous status of the patients) resulted in a marked QT prolongation. Because M cells have a smaller repolarization reserve, increasing ε exerted a larger effect on AP duration in these cells, which resulted in increased V_m gradients and, consequently, increased T-wave amplitudes. These results suggest that changes of late I_{Na}, caused by the p.R689H or p.R689C variants, may exert significant repercussions on the T-wave and the QT interval.

Discussion

The main findings of the present study are summarized as follows: (1) the rare variant p.R689H of $Na_v1.5$ was found in a Russian family with an history of SCD in children, but not in a control cohort of 115 ethnically-matched individuals; (2) both $Na_v1.5$ variants, p.R689H and p.R689C, significantly increased the late I_{Na} recorded in HEK293 cells by a factor of ~1.5 to 2; and (3) simulated pseudo-ECGs indicated that subtle late I_{Na} increases, in the same magnitude as those which were experimentally observed, may lead to QT interval prolongation. The relationship between the increase in late I_{Na} and QT prolongation was found to be nonlinear.

The role of *SCN5A*, the gene encoding $Na_v1.5$, in genetically-determined forms of cardiac arrhythmias has been firmly established over the past decade (1, 2). More than 70 mutations in *SCN5A* have been found in patients with LQTS type 3 (24). In most cases, when the biophysical properties of these LQTS type 3 mutations were studied in cellular expression systems, an increase in late I_{Na} was recorded (25). By delaying the repolarization of the AP, this increased late I_{Na} is an arrhythmogenic factor that can lead to pathological after-depolarizations, and as a consequence prolong the ECG QT interval (25). Similar increases in late I_{Na} were also reported for *SCN5A* variants in SIDS patients (26-28), suggesting that SIDS may, in some cases, be caused by dysfunctional $Na_v1.5$ channels (29). In the case of BrS and genetically-determined cardiac conduction disorders that are linked to *SCN5A* variants, functional investigations have mainly shown loss-of-function of $Na_v1.5$ *via* many different mechanisms (2). In addition, several *SCN5A* variants, found in patients with an "*SCN5A* overlap syndrome" (3), revealed biophysical alterations leading to both LQTS (increased late I_{Na}) and BrS (loss-of-function of I_{Na}).

The current study was initiated by the discovery of the variant p.R689H in the gene *SCN5A* in a family with two cases of SCD in children. This family showed clear signs of altered cardiac conduction with atrio-ventricular block, sinus dysfunction, and bundle branch block (18); but the occurrence of borderline prolonged QT interval in the mother and grand-mother of the proband had also been noticed (Figure 1D). There was no sign of any morphological alterations, hence pointing towards a “pure” functional defect, compatible with an inherited channelopathy (30). The performed biophysical investigations demonstrated that most of the properties of the p.R689H channel were similar to the WT channel. The main difference was a significant doubling of the late I_{Na} (Figure 4), suggesting that heterozygous carriers of this variant may have an *in situ* late I_{Na} that is increased by a factor of ~1.5. It is however obvious that these findings cannot explain the very severe phenotype observed in this family. In addition, these results are difficult to reconcile with the ones from a recent study (13) where no functional expression of this p.R689H variant was observed. We can only speculate on the fact that experimental details such as the plasmids or cells used may be at the origin of this discrepancy.

We also investigated the properties of the p.R689C variant, since it was recently reported in a cohort of 2’500 patients with LQTS (8), and it altered the same Arg-689 residue. In this case, the late I_{Na} was also found to be increased with the p.R689C variant, which is consistent with its occurrence in LQTS patients (8). It is surprising that the substitution of Arg-689 in two residues with different properties (histidine and cysteine) lead both to similar alterations. The detailed roles of the intracellular loop linking the domain I to the domain II of $Na_v1.5$ where these variants are located are not known. It binds to regulatory proteins such as 14-3-3 and calmodulin kinase II (31), and

has been found to be the site of many phosphorylation events (32). Altogether, these findings suggest that small chemical and structural changes of this domain may influence the late I_{Na}. Here, there is also an interesting analogy with the findings reported by Rivolta et al. (23) who have observed an increased late I_{Na} caused by the substitutions of Tyr-1795 also into either histidine or cysteine. The p.Y1795H finding was unexpected since this variant was linked to BrS (23).

It can be assumed that the late I_{Na}, generated by WT channels in human ventricular myocytes, is ~0.1% of the peak transient I_{Na} (33). This is similar to what is found in the expression system of the current study (see Figure 4B). This would correspond to ~50 pA for a typical cardiomyocyte (33). One of the questions that can be raised is whether such a small late I_{Na} increase, caused by one of these two variants, i.e. ~25 pA in a heterologous carrier, may have measurable consequences. In the computer simulations (Figure 5), introducing a late I_{Na} at increasing levels and of comparable magnitude had manifest effects on AP and QT interval duration. These observations are in line with previous computational studies on late I_{Na} and the LQTS type 3 syndrome that were conducted with different cellular models (21, 34). Despite the limitation that late I_{Na} is absent in the original TNNP model, the simulations qualitatively suggest that an increased late I_{Na} of this amplitude may result in measurable changes of the QT interval and, in parallel, an increased risk for arrhythmias.

The findings of the present study are also reminiscent of several recent works that suggest functional effects of similar subtly-increased late I_{Na}. The variant p.S1103Y that is found with an allelic frequency of ~13% in African Americans (16), also increases the late I_{Na} by a factor of ~1.4 (35). This variant has been associated with an increased risk for arrhythmias that are linked to hypokalemia and drugs (35), SIDS (36, 37), and

implantable cardio-defibrillator events in African Americans (38). Also of importance, when tested with more acidic intracellular pH, the variant p.S1103Y generated a late I_{Na} that was markedly increased to ~5% of the peak I_{Na}. Note that no increase in late I_{Na} at more acidotic pH was observed with the p.R689H variant (Figure 4B). In another study that investigated eight *SCN5A* variants, found in SIDS cases (28), significant increases in late I_{Na} were found for five of them. Interestingly, the variant p.R680H, which is located close to the Arg-689 from the current work, showed an increased late I_{Na} only under intracellular acidotic conditions or when expressed in the delQ1077 background (28). These recent findings, together with the ones from our current work, strongly suggest that subtle increases in the late I_{Na} may increase the arrhythmogenic risk in individuals carrying such *SCN5A* variants.

It is apparent that the clinical significance of the p.R689H variant in the studied family is not well understood. This family presents with an important clinical heterogeneity with severe arrhythmic events that lead to SCD. One can speculate that other unknown genetic factors are playing a predominant role in this family. The presence of the p.R689H variant could then be considered as a modifier gene that can increase the risk for arrhythmic events since it may reduce the repolarization reserve (39). Based on this finding, it can be postulated that the carriers of this family may be at a higher risk for malignant arrhythmic events during hypokalemia, hypocalcaemia, or administration of drugs inhibiting the hERG potassium channel (39). As a consequence, these patients should avoid these conditions. Another puzzling aspect of this study is the fact that the variant p.R689H has been described two times in cohorts of control individuals (Table 1) and with an allelic frequency of 1/12747 in the exome variant server database (19). One has to notice that there is no clinical data from these “control” carriers, and thus it is not

possible to make any assumption about their ECG QTc interval. Moreover, the size of sampling was higher than estimated population prevalence of LQTS (1:5000 – 1:2000). One can only speculate that these individuals may be more at risk than others in situations that would further decrease the repolarization reserve. In conclusion, it is possible that genetic variants with small effects may, as a consequence, play a significant role in SCD (40).

Acknowledgments

We thank D. Shy for her useful comments of this manuscript.

Conflict of Interest Disclosures

None

Figure legends

Figure 1: Clinical and genetic data of Family P. which carries the p.R689H variant.

A. Pedigree of the family with the proband marked with an arrow. Closed symbols represent clinically-affected family members. Hatched symbols represent asymptomatic mutation carriers. The question mark symbol shows family members who refused clinical and genetic investigations. B. ECG leads II and V1 of proband (III.3) registered at 2 year 5 month; sinusal rhythm 102 bpm, PR prolonged 180 ms, and normal QTc 430 ms. C. Fragment of a 24-hour Holter monitoring the ECG of proband (III.3). Sinus arrest, maximal pause 3.65 s, registered at 1 year 2 month. C. Fragment of ECG of the mother of the proband (II.2). Sinus arrhythmia, 64-71 bpm, PQ 140 ms, QRS 80-110 ms, low QRS voltage in III, aVF leads, QTc 450-485 ms, T-wave elevation 1-2 mm in V_1-V_2.

Figure 2: Electrophysiological characterization of the $Na_v1.5$-R689H and $Na_v1.5$-R689C variants

A. Current traces obtained with a current/voltage protocol (see inset) from $Na_v1.5$-WT, p.R689H, or p.R689C transfected cells. B. I/V relationship from $Na_v1.5$-WT (n=12), p.R689H (n=10), and p.R689C (n=7) transfected cells. No significant differences were observed between all three cases. C. Steady-state activation and inactivation curves. Activation properties were determined from I/V relationships by normalizing peak I_{Na} to driving force and maximal I_{Na}. Parameters for the steady-state activation and the voltage-dependence of steady state inactivation (25-ms test pulse to -20 mV after a 500 ms conditioning pre-pulse) are summarized in Table 3 (WT n =11, p.R689H n = 10, P.R689C n = 7). D. Fast inactivation, plotted as the rapid decaying component τ as a function of V_m for WT, p.R689H, and p.R689C I_{Na} (WT n = 11, p.R689H n = 10, p.R689C

n = 7). E. Recovery from inactivation (protocol in inset) was fitted, using a bi-exponential function; time constants and relative weights on averaged data are as follows: for WT, τ_{fast} = 168.9±29.3 s, a_{fast} = 17.41±0.8 , τ_{slow} =12.15±0.36 ms, a_{slow} = 0.91±0.02 (n = 11); for p.R689H, τ_{fast} = 187.9±24.3 s, a_{fast} = 15.1±2.2, τ_{slow} =12.33±0.27 ms, a_{slow} = 0.92±0.02 (n = 10); for p.R689C, τ_{fast} = 148.2±13.6 s, a_{fast} = 17.95±1.1 , τ_{slow} = 12.33±0.27 ms, a_{slow} = 0.89±0.01 (n = 7). F. Time dependence of the onset of slow inactivation was measured using a two-pulse protocol (see inset), and was fitted using a mono-exponential function (τ = 0.7±0.17 s for WT, τ = 0.9±0.2 s for p.R689H, τ = 0.96±0.21 s for p.R689H) (n = 7 to 11).

Figure 3: $Na_v1.5$-R689H dependence on high frequencies and pH.

A. Superposition of 20 current traces, obtained with a -20mV pulse for 500 ms, and corresponding to 20 stimuli that are repeated at two different frequencies (0.5 Hz and 2 Hz) for WT and p.R689H variant. B. Graphical representation of the normalized peak I_{Na} at 20 different stimuli using an intracellular solution with a pH = 7.2 or 6.7. No significant differences in the I_{Na} peak were observed between WT and the p.R689H variant for both frequencies at an acidotic or baseline pH.

Figure 4: Analysis of late current of $Na_v1.5$-R689H and $Na_v1.5$-R689C variants.

A. Representative TTX-sensitive traces showing increased late sodium current (late I_{Na}) for p.R689H and p.R689C compared to WT under intracellular baseline pH conditions. The corresponding peaks I_{Na} were -4890 pA for WT, -5589 pA for p.R689H, and -5132 pA for p.R689C. B. Summary data of late I_{Na} from TTX-sensitive traces, normalized to peak I_{Na} for pH = 7.2 (values in Table 3). Late I_{Na} was measured as the mean current

between 250 and 300 ms, after the initiation of the pulse. C. Summary data of late I_{Na} from WT and p.R689H TTX-sensitive traces, normalized to peak I_{Na} with an acidotic pH (6.7).

Figure 5: Transmural conduction in the TNNP model and corresponding pseudo-ECGs.

A. Schematic of the transmural cable (top), action potentials registered in the middle of the endocardial, mid-myocardial, and epicardial segments (left), and reconstructed pseudo-ECGs (right) for 0%, 0.1%, and 0.15% late I_{Na} (ε=0, 0.00075 and 0.001125), respectively. B. QT interval in the pseudo-ECG as a function of increasing late I_{Na}.

Tables

Variant and refSNP	Clinical phenotype	Ethnical background	Functional characterization	Reference
p.R689H - rs199473145	BrS	Japanese	No functional test	(14)
	BrS/SQTS	Chinese	No I_{Na} in HEK293 cells	(13)
	LQTS	n/a	No functional test	(15)
	Control	Hispanic	No functional test	(16)
	Control (rare)	Not known	No functional test	(17)
	SCD	Russian	This study	This study
p.R689C - rs199473580	LQTS	Not known	No functional test	(8)
	Not relevant	Not relevant	This study	This study

Table 1: Previously published studies, and data from this study, describing the occurrence of the p.R689H and p.R689C variants in cases with arrhythmias and individuals from control cohorts.

Age	Heart rate (bpm)	QTc (ms)	Max pause (ms)	Other findings
3 days old	95-194	400-430	780	-
5 months old	66-197	400-420	840	Syncope
9 months old	89-191	400-430	1100	Sinus arrhythmia
1 year old	71-191	400-425	1200	Sinus arrhythmia, AVB (I)*
1 y. 2m. old	46-192	400-420	3250	Sinus arrhythmia, AVB (I)*
1 y. 6 m. old	53-180	400-430	4950	AVB (I)*, supraventricular extra-systole, RBBB, permanent pacemaker was implanted

Table 2: Age-dependent conduction disturbances, registered from a 24-hour ECG monitoring in proband (III.3, Fig. 1A) who carries the p.R689H mutation; * PQ interval up to 200 ms at night time, registered by Holter Monitoring

	Experimental Data			I_{Na} from TNNP model			
	WT	R689H	R689C	ε = 0	ε = 0.00075	ε = 1.5* 0.00075	ε = 2* 0.00075
Activation	$V_{1/2}$ = -29.8±0.6 K = 5.33±0.18	$V_{1/2}$ = -30.5±0.7 K = 5.43±0.23	$V_{1/2}$ = -29.7±0.8 K = 5.21±0.3	$V_{1/2}$ = -42.3 K = 4.9	$V_{1/2}$ = -42.3 K = 4.9	$V_{1/2}$ = -42.3 K = 4.9	$V_{1/2}$ = -42.3 K = 4.9
Inactivation	$V_{1/2}$ = -72.2±0.5 K = 5.87±0.36	$V_{1/2}$ = -72.8±0.7 K = 5.94±0.40	$V_{1/2}$ = -72.4±0.8 K = 5.83±0.50	$V_{1/2}$ = -84.2 K = 6.1	$V_{1/2}$ = -84.2 K = 6.1	$V_{1/2}$ = -84.2 K = 6.1	$V_{1/2}$ = -84.2 K = 6.1
Late I_{Na}	Yes	Yes	Yes	No	Yes	Yes	Yes
Late I_{Na} /peak current (%)	0.095% ± 0.01	0.19% ± 0.03	0.16% ± 0.02	0%	0.1%	0.16%	0.21%

Table 3: Biophysical I_{Na} parameters from the experiments and simulations. The factor ε is used to simulate a late I_{Na} that does not inactivate (see Material and Methods). Note that the experimental data were not corrected for the liquid junction potential, thus explaining the 16-17 mV difference with the simulated values.

List of References

(1) Priori SG. The fifteen years of discoveries that shaped molecular electrophysiology: time for appraisal. Circ Res 2010;107:451-6.

(2) Wilde AAM, Brugada R. Phenotypical Manifestations of Mutations in the Genes Encoding Subunits of the Cardiac Sodium Channel. Circ Res 2011;108:884-97.

(3) Remme CA, Wilde AAM, Bezzina CR. Cardiac Sodium Channel Overlap Syndromes: Different Faces of SCN5A Mutations. Trends in Cardiovascular Medicine 2008;18:78-87.

(4) Abriel H. Cardiac sodium channel Nav1.5 and interacting proteins: Physiology and pathophysiology. Journal of Molecular and Cellular Cardiology 2010;48:2-11.

(5) Nuyens D, Stengl M, Dugarmaa S, Rossenbacker T, Compernolle V, Rudy Y et al. Abrupt rate accelerations or premature beats cause life-threatening arrhythmias in mice with long-QT3 syndrome. Nat Med 2001;7:1021-7.

(6) Watanabe H, Yang T, Stroud DM, Lowe JS, Harris L, Atack TC et al. Striking In Vivo Phenotype of a Disease-Associated Human SCN5A Mutation Producing Minimal Changes in Vitro. Circulation 2011;124:1001-11.

(7) Davis RP, Casini S, van den Berg CW, Hoekstra M, Remme CA, Dambrot C et al. Cardiomyocytes Derived from Pluripotent Stem Cells Recapitulate Electrophysiological Characteristics of an Overlap Syndrome of Cardiac Sodium Channel Disease. Circulation 2012;125:3079-91.

(8) Kapplinger JD, Tester DJ, Salisbury BA, Carr JL, Harris-Kerr C, Pollevick GD et al. Spectrum and prevalence of mutations from the first 2,500 consecutive unrelated patients referred for the FAMILION long QT syndrome genetic test. Heart Rhythm 2009;6:1297-303.

(9) Kapplinger JD, Tester DJ, Alders M, Benito B, Berthet M, Brugada J et al. An international compendium of mutations in the SCN5A-encoded cardiac sodium channel in patients referred for Brugada syndrome genetic testing. Heart Rhythm 2010;7:33-46.

(10) Abriel H, Zaklyazminskaya EV. A Modern Approach to Classify Missense Mutations in Cardiac Channelopathy Genes. Circ Cardiovasc Genet 2012;5:487-9.

(11) Kumar P, Henikoff S, Ng PC. Predicting the effects of coding non-synonymous variants on protein function using the SIFT algorithm. Nat Protoc 2009;4:1073-81.

(12) Anonymous. CardioDB. 2013. Ref Type: Online Source

(13) Hong K, Hu J, Yu J, Brugada R. Concomitant Brugada-like and short QT electrocardiogram linked to SCN5A mutation. Eur J Hum Genet 2012;20:1189-92.

(14) Nakajima T, Kaneko Y, Saito A, Irie T, Tange S, Iso T et al. Identification of six novel SCN5A mutations in Japanese patients with Brugada syndrome. Int Heart J 2011;52:27-31.

(15) Napolitano C, Priori SG, Schwartz PJ, Bloise R, Ronchetti E, Nastoli J et al. Genetic testing in the long QT syndrome: development and validation of an efficient approach to genotyping in clinical practice. JAMA 2005;294:2975-80.

(16) Ackerman MJ, Splawski I, Makielski JC, Tester DJ, Will ML, Timothy KW et al. Spectrum and prevalence of cardiac sodium channel variants among black, white, Asian, and Hispanic

individuals: implications for arrhythmogenic susceptibility and Brugada/long QT syndrome genetic testing. Heart Rhythm 2004;1:600-7.

(17) Kapa S, Tester DJ, Salisbury BA, Harris-Kerr C, Pungliya MS, Alders M et al. Genetic Testing for Long-QT Syndrome. Distinguishing Pathogenic Mutations From Benign Variants. Circulation 2009.

(18) Makarov LM, Komoliatova VN, Kolosov VO, Solokhin I. (Sudden death of two sisters in a family with combined progressive impairment of cardiac conduction system). Kardiologiia 2012;52:91-0.

(19) Anonymous. NHLBI Exome sequencing project. 2012 Ref Type: Online Source.

(20) ten Tusscher KHWJ, Noble D, Noble PJ, Panfilov AV. A model for human ventricular tissue. Am J Physiol Heart Circ Physiol 2004;286:H1573-H1589.

(21) Gima K, Rudy Y. Ionic current basis of electrocardiographic waveforms: a model study. Circ Res 2002;90:889-96.

(22) Plonsey R, Barr RC. Bioelectricity: A Quantitative Approach. New York, NY: Plenum Press; 1988.

(23) Rivolta I, Abriel H, Tateyama M, Liu H, Memmi M, Vardas P et al. Inherited Brugada and long QT-3 syndrome mutations of a single residue of the cardiac sodium channel confer distinct channel and clinical phenotypes. J Biol Chem 2001;276:30623-30.

(24) The gene connection for the heart. 2013. Ref Type: Online Source

(25) Moreno JD, Clancy CE. Pathophysiology of the cardiac late Na Current and its potential as a drug target. Journal of Molecular and Cellular Cardiology 2011;52:608-19.

(26) Schwartz PJ, Priori SG, Dumaine R, Napolitano C, Antzelevitch C, Stramba-Badiale M et al. A molecular link between the sudden infant death syndrome and the long- QT syndrome. N Engl J Med 2000;343:262-7.

(27) Ackerman MJ, Siu BL, Sturner WQ, Tester DJ, Valdivia CR, Makielski JC et al. Postmortem molecular analysis of SCN5A defects in sudden infant death syndrome. JAMA 2001;286:2264-9.

(28) Wang DW, Desai RR, Crotti L, Arnestad M, Insolia R, Pedrazzini M et al. Cardiac Sodium Channel Dysfunction in Sudden Infant Death Syndrome. Circulation 2007;115:368-76.

(29) Van Norstrand DW, Ackerman MJ. Genomic risk factors in sudden infant death syndrome. Genome Med 2010;2:86.

(30) Cerrone M, Priori SG. Genetics of sudden death: focus on inherited channelopathies. Eur Heart J 2011;32:2109-18.

(31) Shy D, Gillet L, Abriel H. Cardiac Sodium Channel Nav1.5 Distribution in Myocytes via Interacting Proteins: The Multiple Pool Model. Biochimica et Biophysica Acta (BBA) - Molecular Cell Research 2012;1833:886-94.

(32) Marionneau C, Lichti CF, Lindenbaum P, Charpentier F, Nerbonne JM, Townsend RR et al. Mass Spectrometry-Based Identification of Native Cardiac Nav1.5 Channel alpha Subunit Phosphorylation Sites. J Proteome Res 2012;11:5994-6007.

(33) Maltsev VA, Undrovinas AI. A multi-modal composition of the late Na+ current in human ventricular cardiomyocytes. Cardiovasc Res 2006;69:116-27.

(34) Trenor B, Cardona K, Gomez JF, Rajamani S, Ferrero JM, Jr., Belardinelli L et al. Simulation and mechanistic investigation of the arrhythmogenic role of the late sodium current in human heart failure. PLoS ONE 2012;7:e32659.

(35) Splawski I, Timothy KW, Tateyama M, Clancy CE, Malhotra A, Beggs AH et al. Variant of SCN5A sodium channel implicated in risk of cardiac arrhythmia. Science 2002;297:1333-6.

(36) Plant LD, Bowers PN, Liu Q, Morgan T, Zhang T, State M et al. A common cardiac sodium channel variant associated with sudden infant death in African Americans, SCN5A S1103Y. Journal of Clinical Investigation 2006;116:430-5.

(37) Van Norstrand DW, Tester DJ, Ackerman MJ. Overrepresentation of the proarrhythmic, sudden death predisposing sodium channel polymorphism S1103Y in a population-based cohort of African-American sudden infant death syndrome. Heart Rhythm 2008;5:712-5.

(38) Sun AY, Koontz JI, Shah SH, Piccini JP, Nilsson KR, Craig D et al. The S1103Y Cardiac Sodium Channel Variant Is Associated with ICD Events in African Americans with Heart Failure and Reduced Ejection Fraction. Circ Cardiovasc Genet 2011;4:163-8.

(39) Roden DM. Long QT syndrome: reduced repolarization reserve and the genetic link. Journal of Internal Medicine 2006;259:59-69.

(40) George AL, Jr. Common genetic variants in sudden cardiac death. Heart Rhythm 2009;6:S3-S9.

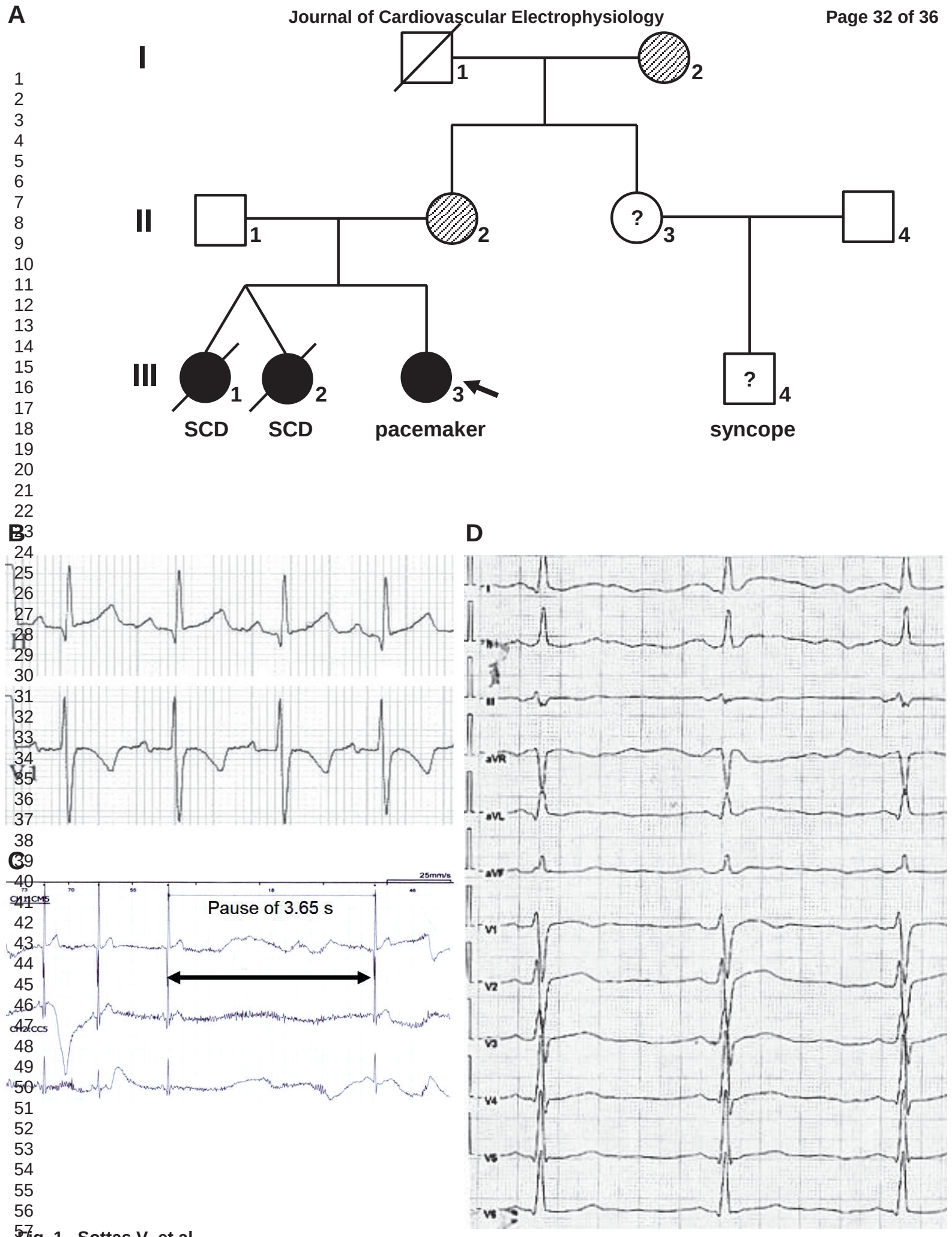

Fig. 1. Sottas V. et al.

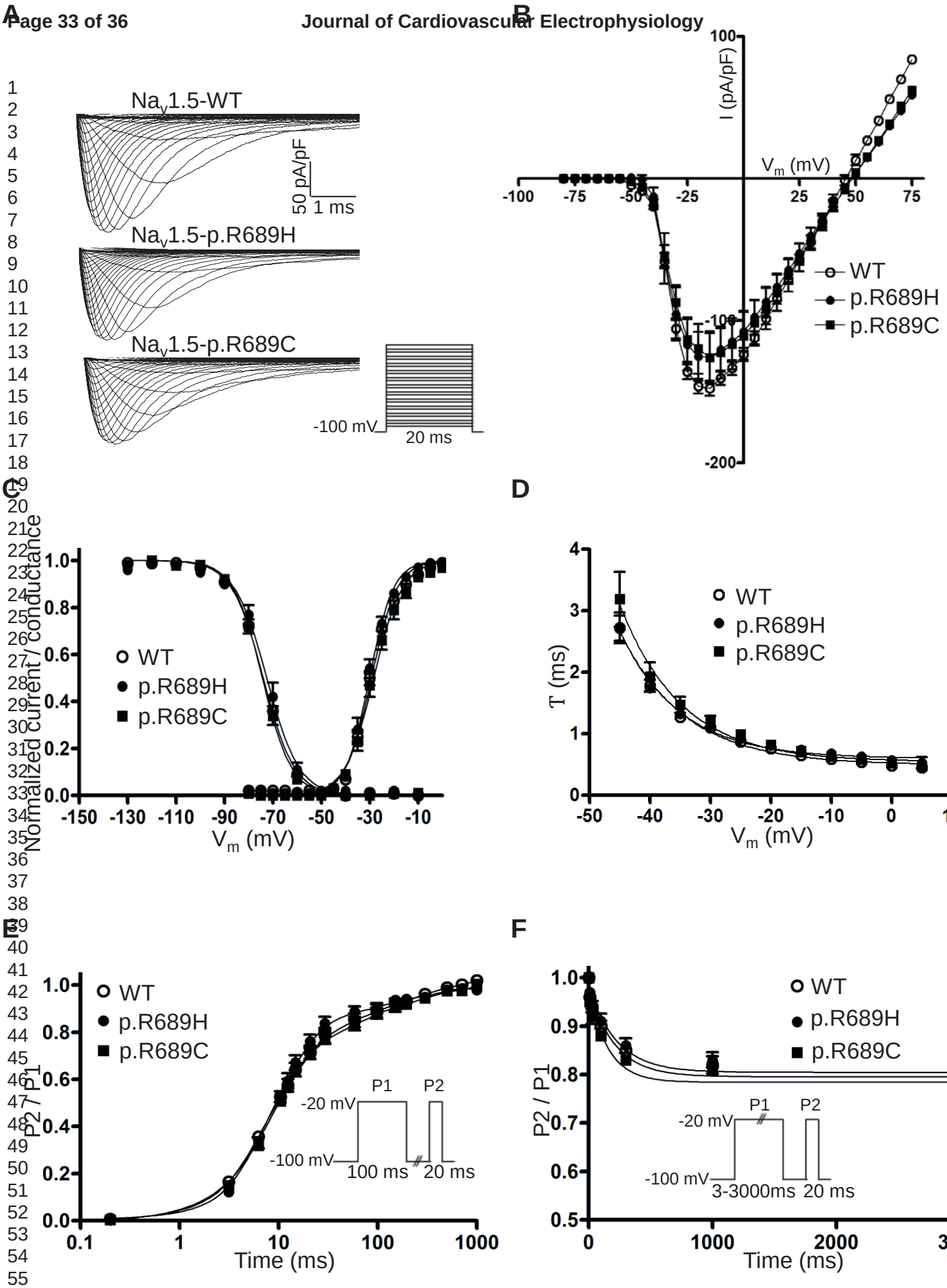

Fig. 2. Sottas V. et al.

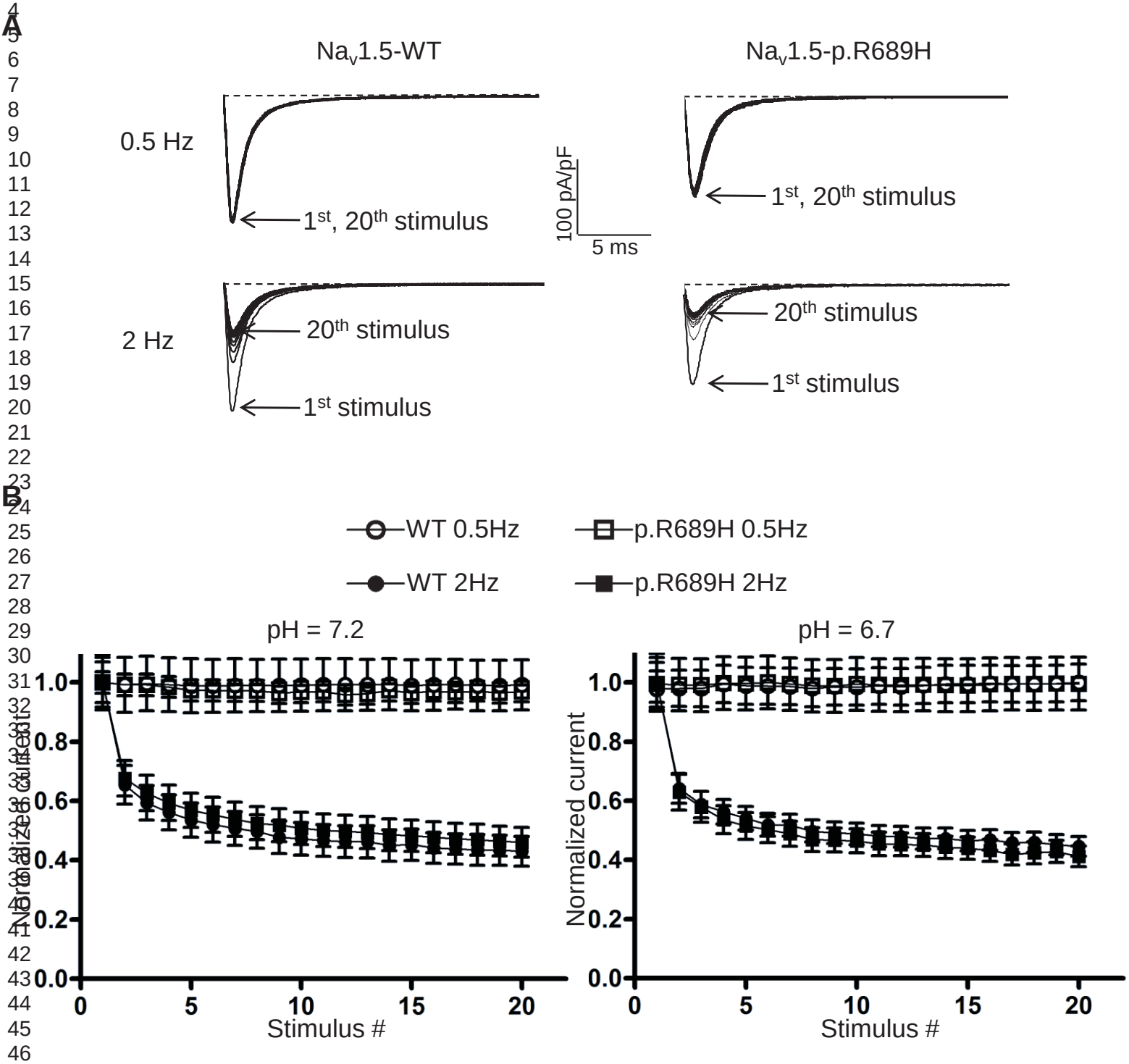

Fig. 3. Sottas V. et al.

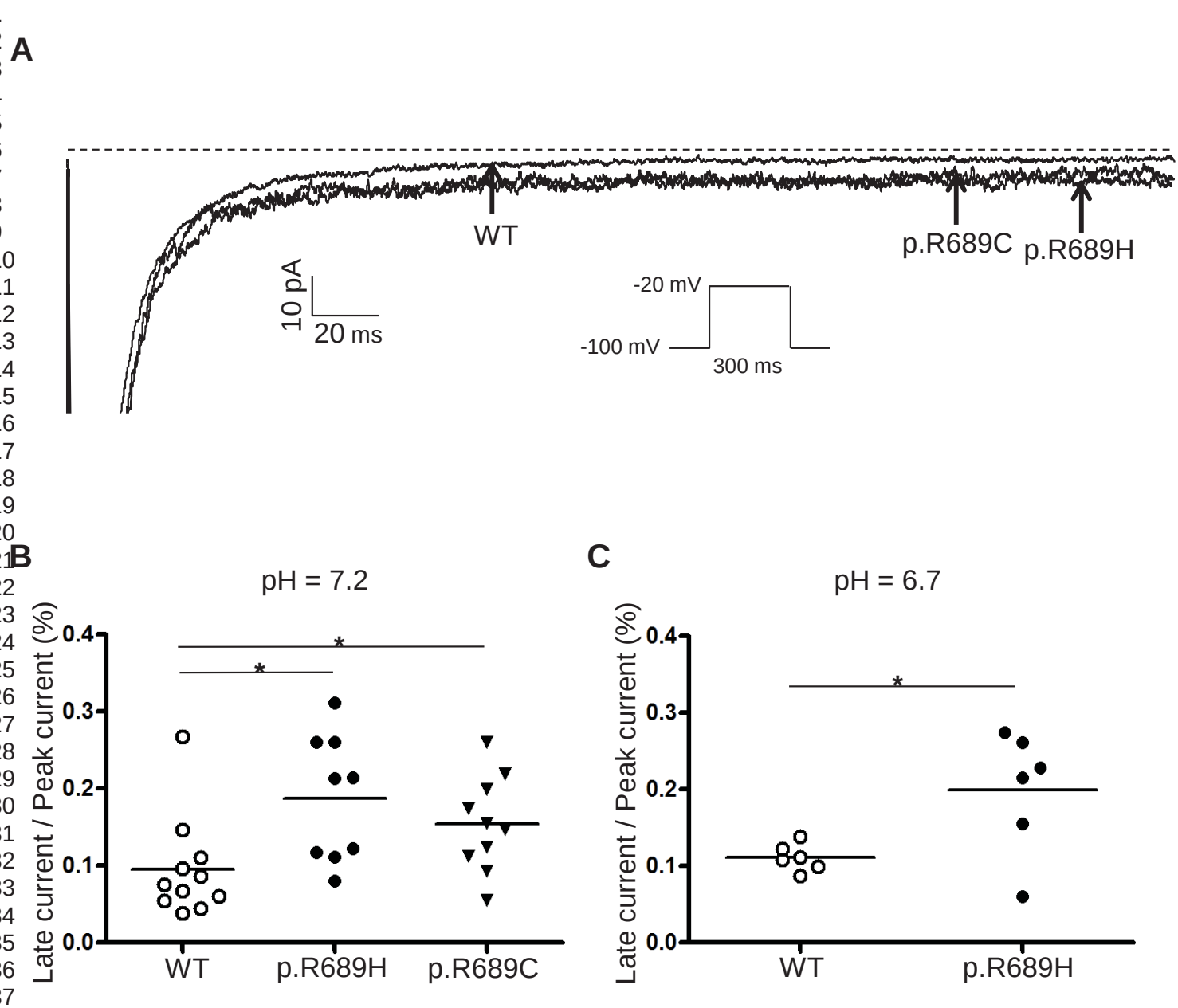

Fig. 4. Sottas V. et al.

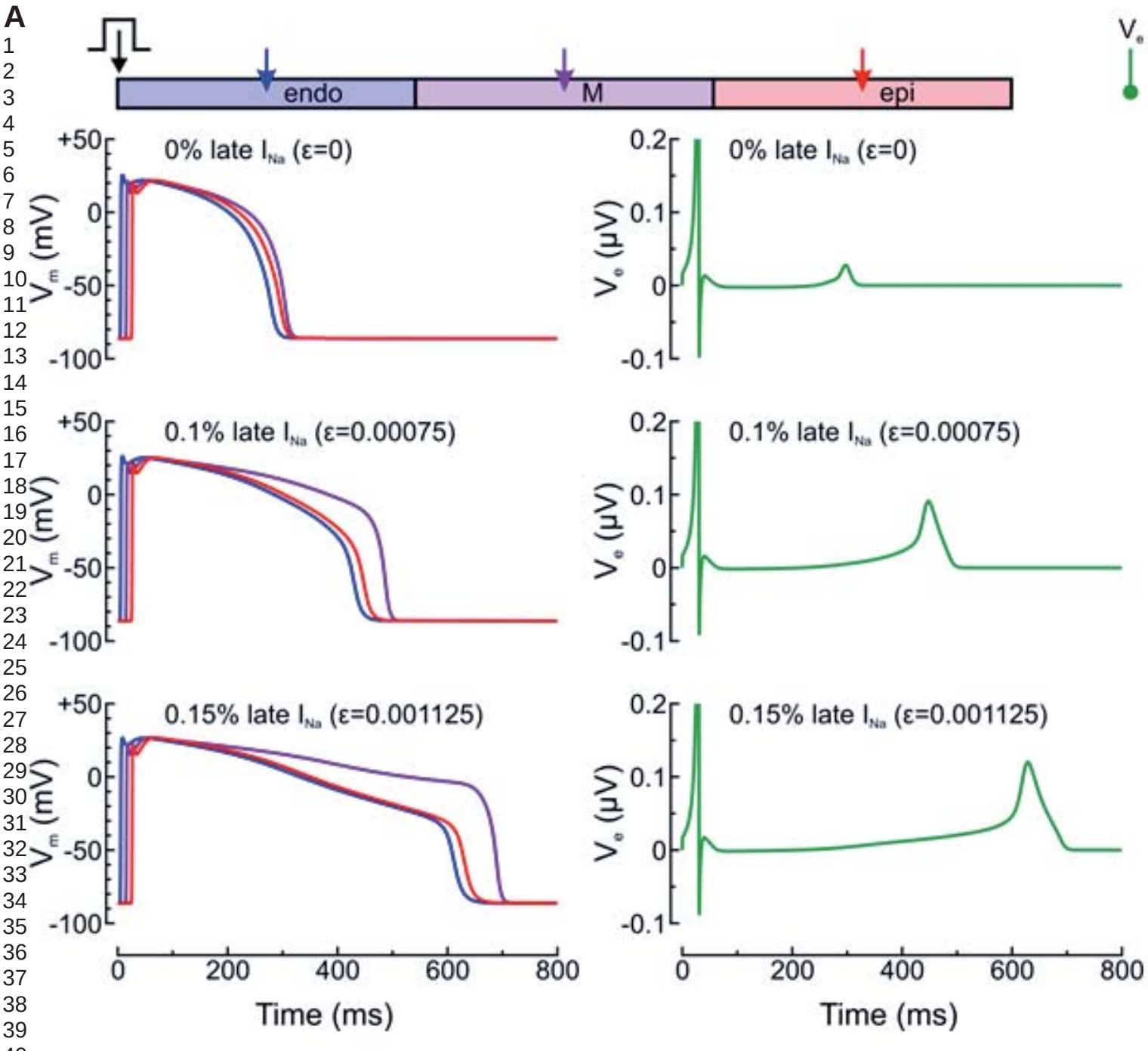

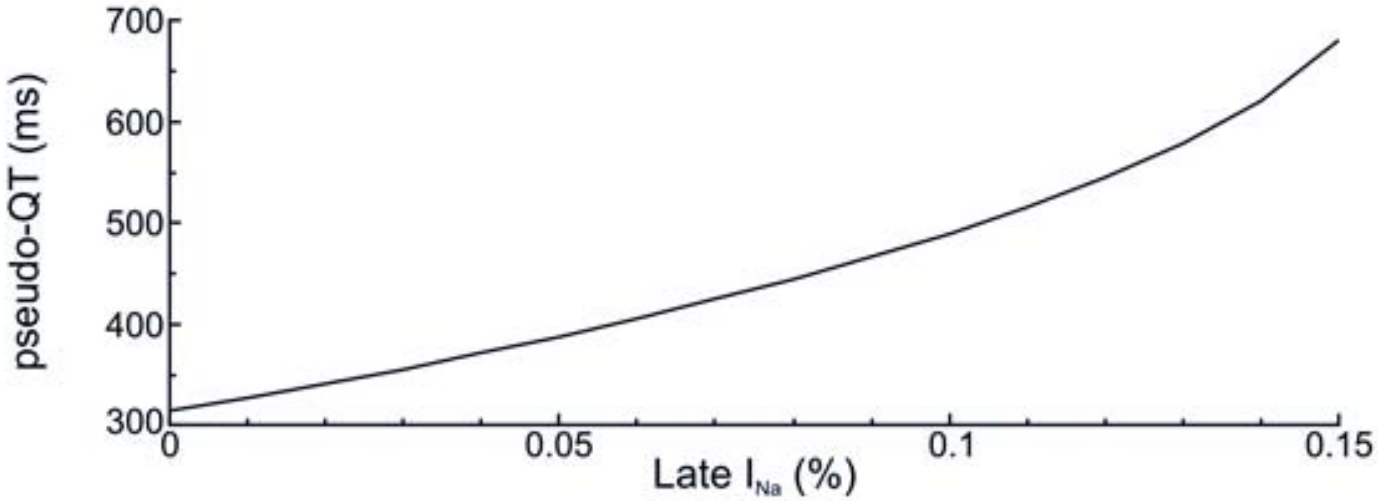

Fig. 5. Sottas V. et al.